Steady-State Electron Transport in Silicon Dioxide Employing Different Electronic Band-Structures

M. Hackel, H. Kosina, and S. Selberherr

Institute for Microelectronics
Technical University of Vienna
Gusshausstrasse 27–29, A-1040 Vienna, Austria

Abstract

A semiclassical Monte Carlo technique is employed to simulate the steady-state electron transport in silicon dioxide at intermediate and high electric fields. The electronic structure is modelled by a single parabolic, by a single nonparabolic as well as an isotropic four-band model. We find that the electronic behavior of silicon dioxide is mainly influenced by a single nonparabolic conduction-band. The injection of electrons into silicon dioxide is also investigated in order to extract the thermalization length of electronic carriers.

I. Introduction

Silicon dioxide is of vital interest for "metal oxide semiconductor" (MOS) technology because of its importance as an insulator for gate electrodes. For "Ultra Large Scale Integrated" (ULSI) circuits the thickness of the insulating film is only comprised of a few nanometers, which results (for typical bias voltages) in a normal field approximately of 1 – 10 megavolts per centimeter (MV/cm). Experimental and theoretical studies give evidence that material breakdown will not occur under the influence of applied field-strengths as high as 20 MV/cm [1][2]. Under these enormous fields, the electronic distribution becomes unstable if the energy being gained from the field can no longer be given to the lattice. Three different scattering events are involved to model the transport behavior of electrons in SiO_2, namely, polar longitudinal optical (LO) phonons, nonpolar optical and nonpolar acoustic phonons [1][3][4][5][6][7][8].

II. The Physical Model

In low electron energy levels, polar longitudinal optical phonons are the dominant scattering process in silicon dioxide. The electrons lose a large amount of energy to the lattice due to a strong interaction of the polar phonon modes via the polarization field of the ions, but at high and intermediate fields they cannot prevent "velocity runaway" or even material destruction. Nonpolar acoustic phonons force electrons to scatter and stabilize the electronic distribution. As electrons reach the threshold for the emission of nonpolar acoustic phonons, the probability of having Bragg reflections (Umklapp-processes) increases keeping electronic carriers from gaining more energy from the field [3][7][9].

III. The Transport Model

In this section we briefly describe our Monte Carlo algorithm to solve the Boltzmann transport equation (BTE). An excellent review on this method is given in [10]. Some minor improvements and differences of this numerical method will be briefly reported here. The equation of motion and the duration of free flight are solved simultaneously by employing a Runge-Kutta algorithm instead of the usual self-scattering scheme. After performing a free flight the scattering process is randomly chosen according to the partial scattering rates. If one scattering process is selected the after-scattering state of the electron is calculated. For nonpolar electron-phonon collisions the polar θ and azimuthal angle ϕ are uniformly distributed [10], whereas the LO phonons favor large angle scattering. To compute the polar angle we use a modified rejection technique with a nonconstant enveloping function. The azimuthal angle of the LO phonons is chosen randomly. Having calculated the state of the scattered electron we perform another free flight till the maximum number of scattering events is reached.

IV. Results

To model the band-structure in SiO_2 we implemented an isotropic four-band model with one nonparabolic (nonparabolicity α) and three parabolic bands [11]

$$\epsilon(1+\alpha\epsilon) = \frac{\hbar^2 k^2}{2m^*} \quad \text{for } 0 \leq k \leq k_{max} \quad \text{band 1,} \tag{1}$$

$$\epsilon = \epsilon_0 \pm \frac{\hbar^2 k^2}{2m^*} \quad \text{for } 0 \leq k \leq k_{max} \quad \text{band 2,3,4.} \tag{2}$$

band	m^* $[m_e\text{-}]$	ϵ_1 $[eV]$	ϵ_2 $[eV]$	k_{max} $[nm^{-1}]$	multiplicity
1	0.50	0.00	5.52	11.54	6
2	1.34	5.52	9.31	11.54	6
3	1.05	7.00	9.00	7.42	12
4	1.05	9.00	11.00	7.42	12

Table 1. Parameters of the four-band model used

The parameters of the band-structure are summarized in Table 1. The data were extracted from band calculations of Chelikovsky and Schlüter [12].

In contrast to the electronic character of bands one and three, the bands two and four show hole-like behavior. The density of states (figure 1) of one parabolic, one nonparabolic and the four-band model are compared, whereas the first bands have the same mass. It is clearly seen for intermediate and high energies that the density of states strongly differs. The main features of a realistic band-structure with two maxima at 5.5 eV and 9 eV and one minimum at 7 eV are well reproduced and strongly influence the electronic distribution at all energies.

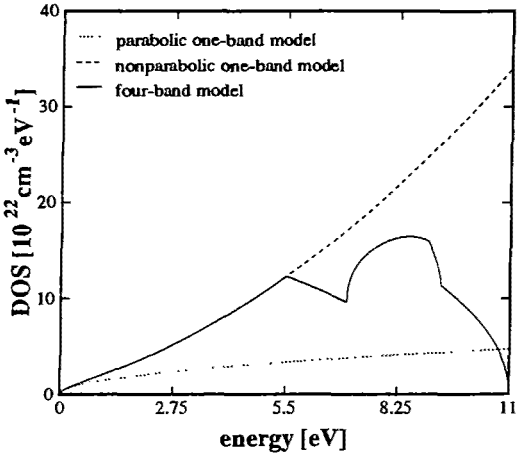

Figure 1. DOS of different band-structures used for SiO_2.

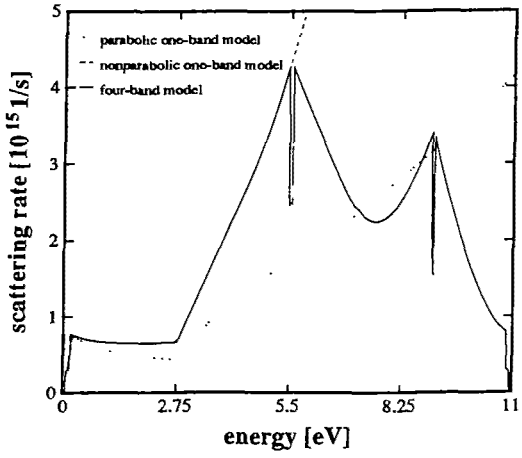

Figure 2. Scattering rates of different band-structures used for SiO_2

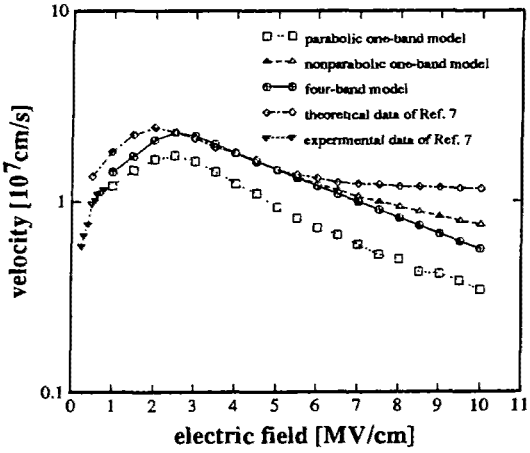

Figure 3. Drift velocity of different band-structures in SiO_2.

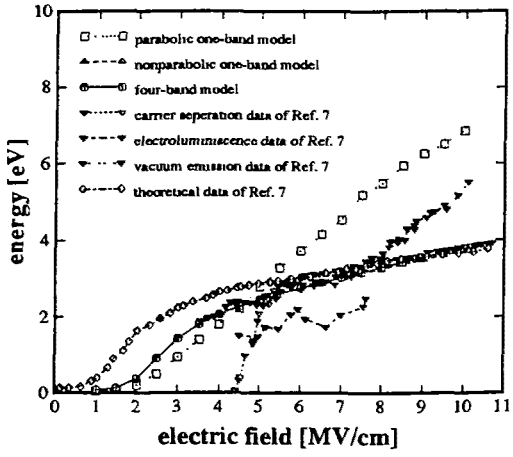

Figure 4. Mean kinetic energy in SiO_2 compared with the data of Ref. 7.

Figure 2 presents the total scattering rate for a temperature of 300 K and compares it with a single conduction-band. Nonpolar acoustic phonons set in at about 2.75 eV as the dominant scattering process (U-process). Compared with one-band models the different character of the four-band model again results in two maxima and one minimum. The discontinuity at the peak reflects the intravalley character of U-processes.

The dependence of the drift velocity of electronic carriers in SiO_2 versus electric field is plotted in figure 3. It increases till U-processes occur. A parabolic one-band model tends to lower velocities, whereas nonparabolicity increases the velocity. The split-off between the nonparabolic band-model and the four-band model is caused by a non-negligible occupancy of the second band at high electric fields. Our data are compared with the results of Fischetti [7][13].

The energy is plotted in figure 4. We observe that a single nonparabolic conduction-band and the four-band model do not exhibit any deviation, moreover, they almost demonstrate

quantitative identical values. Three different techniques have been employed to extract the energy as a function of the applied electric field, namely the carrier-separation technique, the electroluminiscence method and finally the vacuum-emission technique [1],[2],[7].

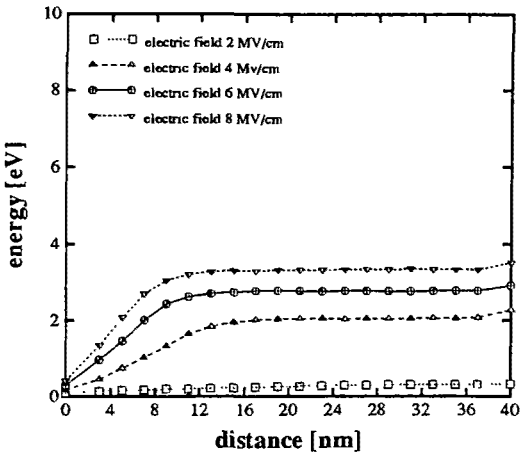

Figure 5. Spatial energy distribution in SiO_2 for electrons injected with 0.1 eV.

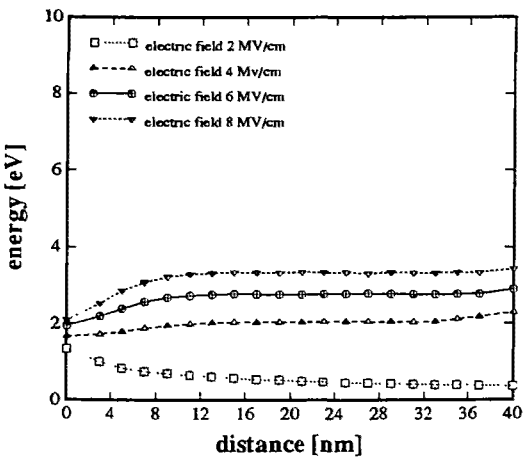

Figure 6. Spatial energy distribution in SiO_2 for electrons injected with 1 eV.

In figure 5 we investigate the thermalization length of electrons in SiO_2 employing one nonparabolic band. Electrons are injected at the left boundary according to an Boltzmann distribution with an average energy of 0.01 eV. We find that the thermalization length is dependent on the applied electric field as well as on the energy of the injected electrons. At low field-strengths the distribution shows that the electrons requires an average distance of about 30 nm to obtain the mean kinetic energy, whereas at high fields the average distance to thermalize is obviously lower than 10 nm. If the average energy of the applied field does not reach the threshold of U-processes the scattering rate is rather low and the mean free path large. Therefore scattering events are rarely resulting in long thermalization lengths. For high fields the mean free path is short and U-processes are dominant favoring large-angle scattering, which thermalize the carriers within few nm.

Figure 6 presents the distribution of electrons in SiO_2 that are injected with 1 eV in average. Again, we observe that the thermalization length of electrons is dependent on the electric field, but shorter than for carriers injected with low energy. The average length for electrons to thermalize is lower than 15 nm. For high fields it is clearly seen that electrons thermalize within 10 nm. In contrast to injected electrons with low energy the probability of suffering U-processes is high leading to a short mean free path and a short thermalization length.

Acknowledgement

The financial support of SIEMENS, Germany, is gratefully acknowledged. The authors are indebted to DIGITAL Equipment Corporation, USA, for providing an excellent computer environment.

References

[1] M.V. Fischetti. *Physical Review Letters*, 53(18):1755–1758, 1984.

[2] M.V. Fischetti and D.J. DiMaria. *Physical Review Letters*, 55(22):2475–2478, 1985.

[3] B.K. Ridley. *Journal of Applied Physics*, 46(3):998–1007, 1975.

[4] W. Porod and D.K. Ferry. *Physical Review Letters*, 54(11):1189–1191, 1985.

[5] H. Köstner Jr. and K. Hübner. *Physica status solidi (b)*, 118:293–301, 1983.

[6] H.-J. Fitting and J.-U. Friemann. *Physica status solidi (a)*, 69:349–358, 1985.

[7] M.V. Fischetti, D.J. DiMaria, S.D. Brorson, T.N. Theis, and J.R. Kirtley. *Physical Review B*, 31(11):8124–8142, 1985.

[8] M.V. Fischetti and D.J. DiMaria. *Solid-State Electronics*, 31(3/4):629–634, 1988.

[9] M. Sparks, D.L. Mills, A.A. Maradudin, L.J. Sham, E. Loh Jr., and D.F. King. *Physical Review B*, 24(6):3519–3536, 1981.

[10] C. Jacoboni and L. Reggiani. *Review Modern Physics*, 55(3):645–705, 1983.

[11] R. Brunetti, C. Jacoboni, F. Venturi, E. Sangiorgi, and B. Ricco. *Solid-State Electronics*, 32(12):1663–1667, 1989.

[12] J.R. Chelikowsky and M. Schlüter. *Physical Review B*, 15(8):4020–4029, 1977.

[13] M.V. Fischetti, S.E. Laux, and D.J. DiMaria. *Applied Surface Science*, 39:578–596, 1989.